JTTEE5 19:328–335
DOI: 10.1007/s11666-009-9441-z
1059-9630/$19.00 © ASM International

Atmospheric Plasma Spraying Low-Temperature Cathode Materials for Solid Oxide Fuel Cells

J. Harris and O. Kesler

(Submitted April 24, 2009; in revised form September 18, 2009)

Atmospheric plasma spraying (APS) is attractive for manufacturing solid oxide fuel cells (SOFCs) because it allows functional layers to be built rapidly with controlled microstructures. The technique allows SOFCs that operate at low temperatures (500-700 °C) to be fabricated by spraying directly onto robust and inexpensive metallic supports. However, standard cathode materials used in commercial SOFCs exhibit high polarization resistances at low operating temperatures. Therefore, alternative cathode materials with high performance at low temperatures are essential to facilitate the use of metallic supports. Coatings of lanthanum strontium cobalt ferrite (LSCF) were fabricated on steel substrates using axial-injection APS. The thickness and microstructure of the coating layers were evaluated, and x-ray diffraction analysis was performed on the coatings to detect material decomposition and the formation of undesired phases in the plasma. These results determined the envelope of plasma spray parameters in which coatings of LSCF can be manufactured, and the range of conditions in which composite cathode coatings could potentially be manufactured.

Keywords atmospheric plasma spray, $La_{0.6}Sr_{0.4}Co_{0.2}Fe_{0.8}O_{3-\delta}$, LSCF, solid oxide fuel cell, x-ray diffraction

1. Introduction

Solid oxide fuel cells (SOFCs) are very efficient devices that electrochemically convert fuel energy into electricity and heat. These devices are well suited as co-generation units for providing electricity and heat to buildings. Replacing existing heat engines with SOFCs could greatly reduce the consumption of fuels, lowering greenhouse gas and pollutant emissions. However, the high cost of manufacturing SOFCs is a major obstacle preventing their widespread use (Ref 1). SOFCs are traditionally made using wet-ceramic techniques such as tape casting and screen printing. These processes require several days to coat, dry and sinter the cathode, electrolyte, and anode layers, and it is difficult to fabricate metal-supported cells with them due to the need to sinter electrolytes at high temperatures (Ref 2) (typically 1400 °C, or ~1000 °C with sintering aids) (Ref 3). Manufacturing costs could be significantly reduced by using plasma spray processes instead of wet-ceramic techniques. SOFCs made by atmospheric plasma spraying (APS) could potentially be made at lower cost because the cells take merely minutes to make, require less expensive equipment, and can be fabricated on low-cost metallic supports.

To date, the majority of SOFCs fabricated by plasma spraying have used lanthanum strontium manganese oxide (LSM) as the cathode material. Researchers have lowered the polarization resistances in plasma-sprayed cathodes operating at intermediate temperatures (700-850 °C) by designing composite electrodes of LSM and yttria-stabilized zirconia (YSZ). However, while these cathodes have lower polarization resistances (R_p) than single-phase LSM cathodes, even lower values of R_p are needed to further improve low-temperature performance at low operating temperatures, below 750 °C (Ref 4, 5). Therefore, better performing cathodes are needed to operate at low temperatures, where degradation will decrease and less expensive materials can be used for supports.

Lanthanum strontium cobalt iron oxide (LSCF) has been extensively studied as a low-temperature SOFC cathode material because it has high mixed ionic and electronic conductivity at low temperatures (Ref 6-12). It has been shown that single-phase LSCF cathodes can have lower polarization resistances than the state-of-the-art LSM-YSZ composite cathode (Ref 13). In addition, the polarization resistances of cathodes can be lowered

This article is an invited paper selected from presentations at the 2009 International Thermal Spray Conference and has been expanded from the original presentation. It is simultaneously published in *Expanding Thermal Spray Performance to New Markets and Applications: Proceedings of the 2009 International Thermal Spray Conference*, Las Vegas, Nevada, USA, May 4-7, 2009, Basil R. Marple, Margaret M. Hyland, Yuk-Chiu Lau, Chang-Jiu Li, Rogerio S. Lima, and Ghislain Montavon, Ed., ASM International, Materials Park, OH, 2009.

J. Harris and **O. Kesler**, Department of Mechanical and Industrial Engineering, University of Toronto, 5 King's College Road, Toronto, ON, Canada. Contact e-mails: jharris@mie.utoronto.ca and kesler@mie.utoronto.ca.

further by combining LSCF with an ionic conductor in a composite. For example, LSCF has been studied in composites with gadolinia- or samaria-doped ceria (GDC or SDC) (Ref 14-16), with an optimum ceria content of 30-50 wt.%, depending on the details of the manufacturing process and on the fuel cell operating temperature. In the majority of these studies, cathodes were fabricated using wet-ceramic methods.

Although wet-ceramic processing has been optimized for LSCF cathodes, few studies (Ref 17-19) have manufactured LSCF coatings by plasma spraying, and LSCF-SDC composite cathodes have not been made via this process. The challenge of plasma spraying composite cathodes is determining the envelope of process parameters with which coatings can be fabricated. In particular, energetic plasmas are needed to melt fluorite-structured ionic conducting materials (Ref 5, 20, 21), but LSCF decomposes easily in high energy plasmas (Ref 17, 19).

This study determines the envelope of plasma spray conditions with which LSCF coatings can be fabricated without measurably decomposing. Knowing the limitations of process parameters specific to LSCF is important so that LSCF-SDC composite cathodes can be fabricated. To maximize the deposition efficiency of SDC, the torch settings would need to be at the upper end of the LSCF envelope if the feedstock consisted of a mixture of LSCF and SDC powders. Therefore, this work focuses on determining the upper end of the plasma energy range in which LSCF coatings can be fabricated as a single phase with no measurable decomposition.

2. Experimental Procedure

2.1 Materials Preparation

Spray-dried lanthanum strontium cobalt iron oxide (LSCF) powder (Inframat Advanced Materials, Farmington, Connecticut) with the composition $La_{0.6}Sr_{0.4}Co_{0.2}Fe_{0.8}O_{3-\delta}$ was used as the plasma spray feedstock. The as-received powder consisted of spherical agglomerates of nanoparticles with a d_{50} (by volume) agglomerate size of 35.7 μm, as determined by laser light scattering (Mastersizer 2000, Malvern Instruments, Worchestershire, UK). Powders were sieved for 8 h and the powder in the $-75+45$ μm sieve size fraction was used for plasma spraying. The sprayed fraction after sieving had a d_{50} (by volume) of 42.71 μm, determined by laser light scattering. A micrograph of the feedstock obtained by scanning electron microscopy (SEM) is shown in Fig. 1. Image analysis was used to verify the size of the agglomerates, and the median particle size of a very small sample was 33.5 ± 12.7 μm.

Coatings were deposited onto 25.4 mm diameter porous ferritic stainless steel substrates during preliminary tests that used plasmas with high power. For subsequent tests, coatings were deposited onto 2 mm thick 50 mm by 50 mm low-carbon steel plates. The steel substrates were sandblasted to increase the surface roughness so that the coatings would easily adhere.

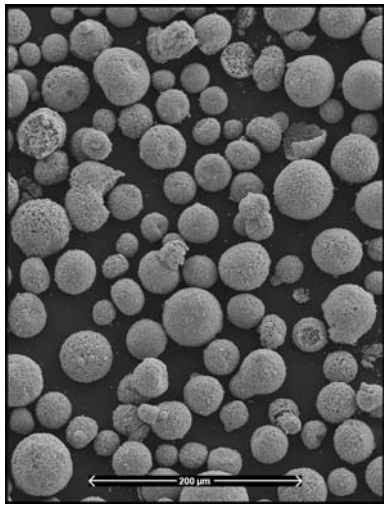

Fig. 1 SEM micrograph of LSCF plasma spray feedstock

2.2 Plasma Spray Processing

Coatings were produced at atmospheric pressure using an Axial III Series 600 plasma torch (Northwest Mettech Corp., North Vancouver, BC, Canada). This torch consists of three cathodes located concentrically around the powder feed line. This arrangement allows the powder to be injected axially into the convergence of three plasma jets, and therefore the feedstock powder is melted uniformly because it is fed directly into the hottest part of the plasma. Additionally, the presence of three converging plasma jets allows the torch to operate with 100% nitrogen. During preliminary experiments with high power plasmas, the torch sprayed the feedstock onto substrates that were mounted on a rotating drum. For subsequent experiments, a robot moved the torch along a raster pattern to coat stationary steel substrates at a standoff distance of 100 mm. The substrates were cooled during spraying by natural convection.

The plasma spraying operating parameters were varied to determine the envelope of conditions in which it is possible to produce coatings of LSCF. These parameters included the plasma gas flow rate, the plasma gas composition, the arc current, and the nozzle size.

2.3 Characterization

The phases present in the coating were determined by x-ray diffraction (XRD), using a Phillips PW 1830 HT diffractometer (PANalytical B.V., Almelo, Netherlands) with a Cu-anode x-ray tube. The incident Bragg angle (2θ) was varied from 20° to 70°. Diffraction patterns of the coatings were compared to the diffraction pattern of the LSCF feedstock powder, shown in Fig. 2(a). Unidentified peaks were identified using the International Centre for Diffraction Data powder diffraction file (2005).

Cross sections of coatings were examined with a scanning electron microscope (Hitachi S-2500, Hitachi High Technologies America, Pleasanton, California) using a secondary electron detector. A tungsten filament was used as the electron source, and the accelerating voltage was

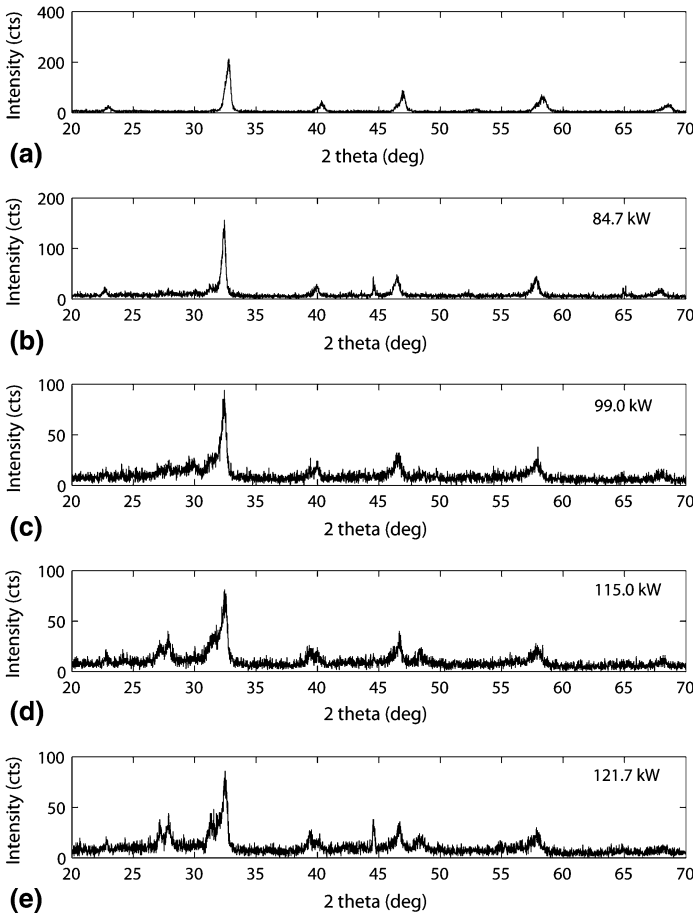

Fig. 2 XRD diffraction patterns of (a) LSCF feedstock powder and of LSCF coatings produced using plasmas with (b) 40% nitrogen, (c) 60% nitrogen, (d) 80% nitrogen, and (e) 100% nitrogen (balance argon)

20 kV. The samples were cut with a diamond saw, mounted in a low-viscosity epoxy, ground with diamond grinding discs, and polished with diamond suspensions.

3. Results and Discussion

3.1 Plasma Gas Composition

3.1.1 Preliminary Tests with High Power (84.7-121.7 kW) Plasmas. LSCF coatings were deposited onto porous stainless steel substrates using the process parameters listed in Table 1. Plasma gases consisted of argon-nitrogen mixtures. The plasma power was controlled by varying the composition of the plasma gas from 40% to 100% nitrogen. The phases of the LSCF coatings were analyzed for possible decomposition, with the XRD patterns of the coatings shown in Fig. 2(b-e).

All preliminary LSCF coatings partially decomposed during plasma spraying, although the primary LSCF peak was still the highest peak in XRD scans. A peak at approximately $2\theta = 27.7°$ appeared in the patterns of all four coatings. This peak corresponds to the primary peak for cubic lanthanum oxide ($2\theta = 27.96°$, ICDD PDF#01-089-4016).

Table 1 Values of plasma spray process parameters during preliminary tests with high power (≥40% nitrogen) and low power (<40% nitrogen) plasma gas compositions

Parameter	High power plasmas	Low power plasmas
Plasma gas flow rate, slpm	200	200
Torch arc current, A per cathode	220	200
Powder feed rate, g/min	20.0	20.0
Nozzle size, mm	12.7 (½ in.)	12.7 (½ in.)
Standoff distance, mm	100	100
Average electrode voltage, V	120-184	82.3-97.8
Total plasma power, kW	84.7-121.7	49.1-59.2
Torch speed relative to substrate, m/s	5.8	0.423
Scanning step per pass, mm	n/a	5.4

The intensity of the 27.7° peak relative to the intensity of the primary LSCF peak increased with higher nitrogen content in the plasma, as shown in Fig. 3, which illustrates that LSCF decomposes more when plasmas with higher powers are used. Other non-LSCF peaks were detected in some of the coatings, but they were not measurable for all coatings. For instance, a peak corresponding to hexagonal lanthanum oxide at $2\theta = 29.98°$ (ICDD PDF#01-083-1344) was measured in a coating produced with a 60% nitrogen

plasma. Although this peak can be visually seen in the diffraction patterns for other coatings, the computer software could not accurately quantify the peak intensities because the peaks overlap each other.

Additionally, the peaks of the XRD patterns shown in Fig. 2(b-e) are shifted to slightly lower angles compared to the feedstock peaks in Fig. 2(a). This is likely a consequence of tensile quenching stresses formed during solidification of the coatings onto the substrate.

3.1.2 Lower Energy (49.1-59.2 kW) Plasmas. LSCF coatings were plasma sprayed onto low-carbon steel substrates using the process parameters in Table 1 and low-nitrogen plasma gas compositions. When 20% nitrogen was used in the plasma gas, the coating material decomposed, and a hexagonal lanthanum oxide peak at $2\theta = 29.9°$ with an intensity of 22% relative to the main LSCF peak was measured by XRD, as shown in Fig. 4(a). With a plasma gas containing 10% nitrogen, LSCF coatings were deposited without measurable decomposition: only LSCF peaks were present in the resulting XRD patterns, as shown in Fig. 4(b).

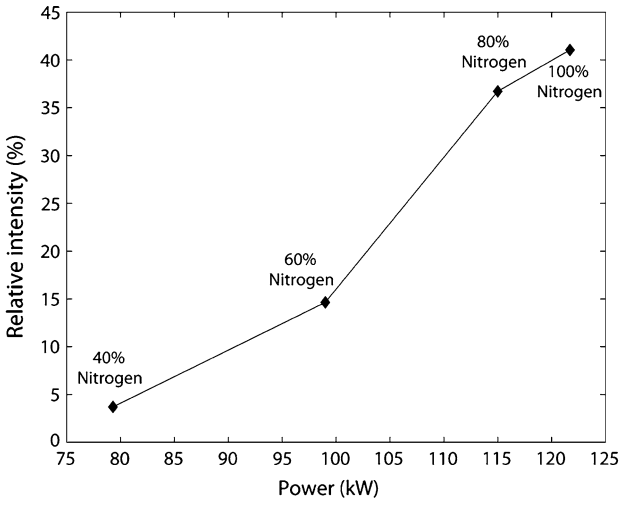

Fig. 3 Intensity of the $2\theta = 27.7°$ diffraction peak relative to the primary LSCF peak as a function of plasma power

3.2 Arc Current and Plasma Gas Flow Rate

The arc current and plasma gas flow rate were varied to determine how these parameters affect the phase of the deposited LSCF coating. In these experiments, the primary hexagonal lanthanum oxide (ICDD #01-083-1344) peak at $2\theta = 29.9°$ was observed and measured in XRD patterns. Plasma spray process parameters and the resulting relative intensity of the lanthanum oxide peak are summarized in Table 2. LSCF decomposed less when lower arc currents were used and when lower plasma gas flow rates were used.

Table 2 Plasma spray process parameters and resultant intensity of decomposed hexagonal La_2O_3 phase relative to that of the LSCF phase

Plasma gas composition		Plasma gas flow rate, slpm	Arc current per cathode, A	Relative intensity of $2\theta = 29.9°$ peak, %
% N_2	% Ar			
20	80	200	200	22.44
20	80	250	200	26.07
20	80	200	150	18.93

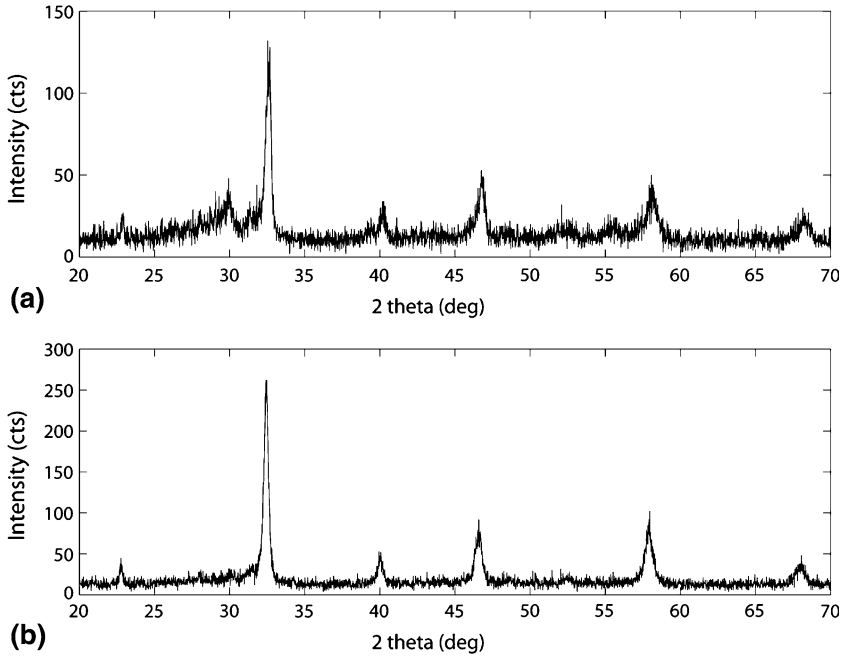

Fig. 4 XRD diffraction patterns of LSCF coatings produced using plasmas with (a) 20% nitrogen, (b) 10% nitrogen (balance argon)

The affect of lower arc current agrees with a study done by Monterrubio-Badillo et al., which concluded that high current increases the gas enthalpy, assisting decomposition (Ref 22). The affect of gas flow, however, contrasts the conclusions of Monterrubio-Badiollo et al., who found that higher plasma gas flow decreased decomposition because it increased the particle velocity and reduced the residence time (Ref 22). In our study, we used 20% nitrogen plasma gas compositions; consequently, increasing the gas flow rate resulted in a higher plasma power that facilitated decomposition. To separate the effect of plasma power from that of residence time, the effect of nozzle size on the resulting coating composition was therefore studied in order to control the particle velocity separately from the plasma power.

3.3 Nozzle Size

The diffraction patterns in Fig. 5 illustrate the effect of the plasma torch nozzle size. These coatings were produced with a 20% N_2/80% Ar plasma flowing at 250 slpm with arc currents of 150 A per cathode. With a large 1/2″ (~12.7 mm) nozzle, some material decomposed, as indicated by the higher intensity around the 30° Bragg angle (Fig. 5a). On the other hand, a smaller 5/16″ (~8 mm) nozzle produced a higher velocity and lower residence time. The coating produced with these conditions did not decompose in the plasma, as indicated by the diffraction pattern in Fig. 5(b).

To better define the envelope of process conditions, LSCF coatings were fabricated using a 5/16″ (~8 mm) nozzle and plasmas with higher power. The intensity is somewhat high between 27° and 30° in the XRD pattern of a coating produced with a 30% nitrogen plasma, as shown in Fig. 6(b). The LSCF feedstock potentially decomposed during processing, although a peak of a secondary phase cannot be identified in the diffraction pattern. Further increasing the nitrogen content resulted in measurable decomposition: the diffraction pattern of a coating produced with a 40% nitrogen plasma has a secondary phase peak at $2\theta = 29.6°$ with an intensity of 14% relative to the primary LSCF peak (Fig. 6c).

Additionally, one coating was produced using a plasma gas mixture of 10% hydrogen and 90% argon, and its XRD pattern is shown in Fig. 6(d). Interestingly, there is no measurable decomposition in this coating within the approximately 5 wt.% detection threshold of XRD. This contrasts the results of studies that have reported that other perovskite cathode materials decompose when any amount of hydrogen is used in the plasma gas (Ref 1, 20), for the plasma gas flow rates and compositions and nozzle sizes examined in those studies.

From the perspective of kinetics and thermodynamics, using a smaller nozzle limits the decomposition of LSCF kinetically. Using a small nozzle increases the particle velocity, and therefore reduces the residence time of the LSCF in the plasma. Therefore, the LSCF may not have sufficient time to decompose, even if the plasma has sufficient energy to thermodynamically favor decomposition.

3.4 Pretreatment of Feedstock

Coatings were also plasma sprayed using an LSCF feedstock powder that was thermally pretreated by

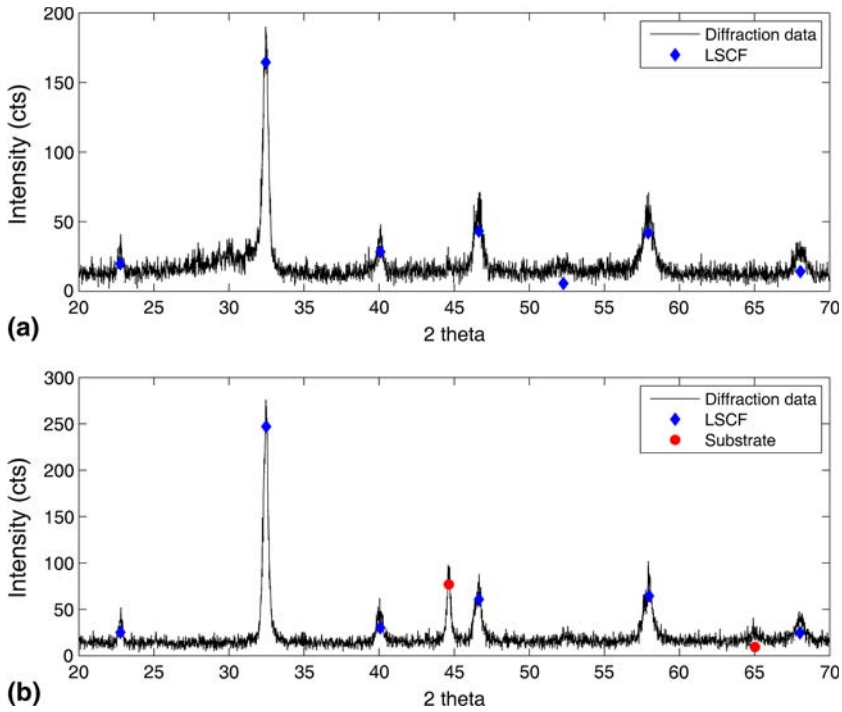

Fig. 5 X-ray diffraction pattern of LSCF coating produced with (a) 1/2″ (~12.7 mm) torch nozzle, (b) 5/16″ (~8 mm) torch nozzle

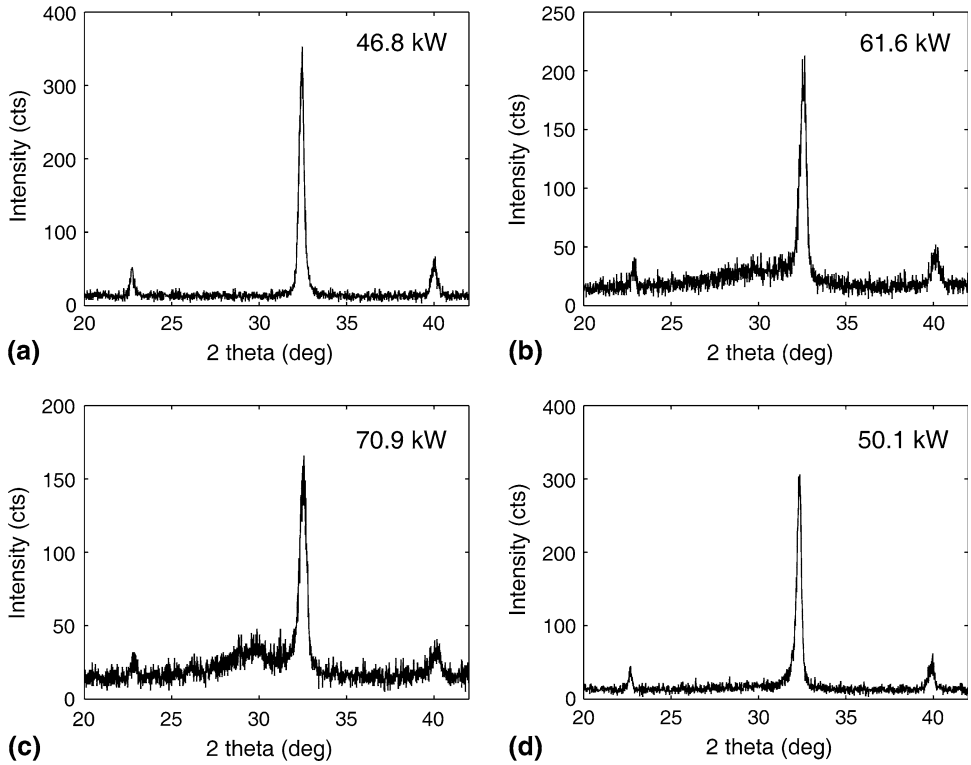

Fig. 6 X-ray diffraction patterns of LSCF coatings produced with a 5/16″ (~8 mm) nozzle, 250 slm gas flow, 150 A per cathode, and plasma gas consisting of argon and (a) 20% nitrogen, (b) 30% nitrogen, (c) 40% nitrogen, and (d) 10% hydrogen

calcination, and the phases of the coatings were evaluated by XRD. For these experiments, the feedstock powder was calcined for 5.5 h at 1238 °C. This temperature was sufficiently high to partially sinter the spray-dried agglomerates, yet it preserved the nanostructure of the particles, as shown in the micrographs in Fig. 7(a, b). LSCF coatings were produced with plasmas consisting of gas mixtures up to 100% nitrogen and having powers up to 123.0 kW. No measurable quantities of undesired phases were observed in XRD patterns of these coatings produced from the calcined LSCF feedstock, as shown in Fig. 8.

The diffraction pattern shown in Fig. 8 is remarkably different from the diffraction pattern in Fig. 2(e), which was produced using similar plasma spray parameters and a noncalcined feedstock. It is hypothesized that the noncalcined spray-dried agglomerates were held together loosely and thus disintegrated in the plasma into very fine particles. Therefore, these particles would have a very large surface area exposed to the plasma. This means that if decomposition occurred in only thin layers on the surfaces of the fine particles, a substantial fraction of the material would decompose. In contrast, it is expected that the calcined agglomerates adhered together well and did not break up in the plasma. In this case, the fraction of decomposed LSCF would be below the XRD detection threshold if decomposition occurred in only thin layers on the surfaces of calcined agglomerates.

3.5 Cross Section and Coating Thickness

The cross section of a typical plasma-sprayed LSCF coating is shown in Fig. 9 This coating was 44 ± 7 μm in thickness as determined by image analysis, and the microstructure is somewhat porous. A low plasma energy (40.2 kW) was used to produce the coating, and thus porosity was likely formed because some LSCF particles did not completely melt in the plasma. The porosity is beneficial for the facilitation of gas transport to the reaction sites in the cathode and also increases the reaction surface area on which the reaction can take place on the mixed-conducting LSCF. This effect of partial melting was observed by White et al. in studies of LSM coatings (Ref 1).

4. Conclusions

Moderately porous LSCF coatings were fabricated by APS using nitrogen and argon plasma gases. As shown by XRD, noncalcined LSCF decomposes into undesired phases when high plasma powers are used. The plasma power and decomposition can be reduced by decreasing the nitrogen content in the plasma gas. Decomposition can also be reduced by lowering the arc current and by decreasing the plasma gas flow rate. However, even with a low current and low plasma gas flow rate, unwanted

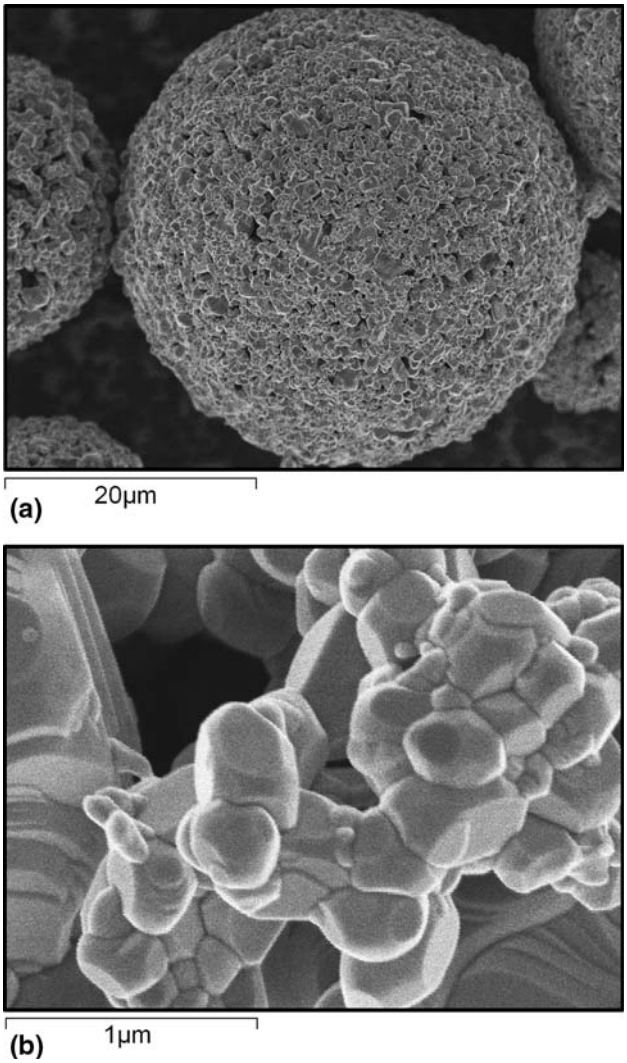

Fig. 7 Micrograph of LSCF plasma spray feedstock after calcination at 1238 °C for 5.5 h. (a) 2500× magnification and (b) 50,000× magnification

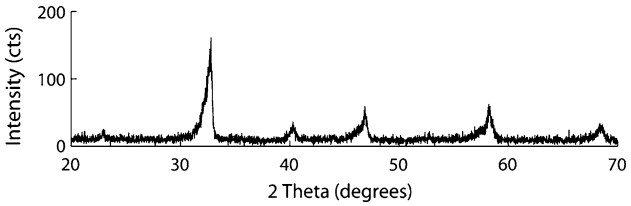

Fig. 8 XRD pattern of LSCF coating produced using a calcined feedstock, a 100% N_2 plasma flowing at 200 slpm with an arc current of 250 A per cathode, and a nozzle size of 1/2″ (~12.7 mm)

phases were detected when 20% nitrogen and a 1/2″ (~12.7 mm) nozzle were used. Coatings that did not decompose were fabricated by lowering the nitrogen content to 10%. Alternatively, two strategies were used to produce single-phase LSCF coatings. First, the particle velocity was increased by using a smaller 5/16″ (~8 mm) torch nozzle to decrease the particle residence time, allowing the use of plasmas with up to 20% nitrogen. Second, the coherence of the agglomerates in the feedstock was increased by calcining the powder prior to spraying. This allowed the use of high power plasmas with up to 100% nitrogen with no measurable decomposition.

These results define the envelope for which single-phase LSCF can be plasma sprayed using argon and nitrogen mixtures, and this envelope of parameters will guide the selection of conditions for the plasma spraying of composite LSCF-SDC SOFC cathodes.

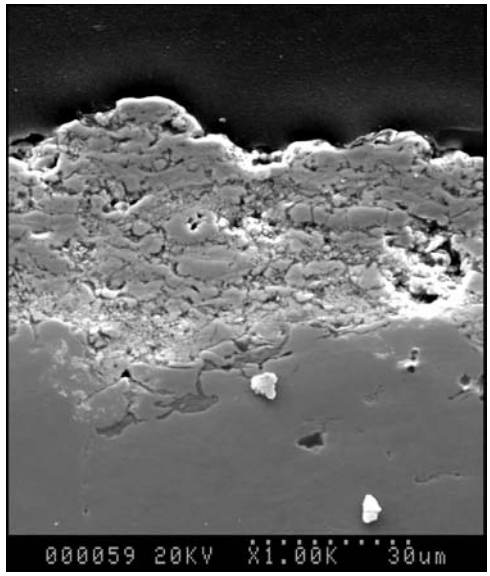

Fig. 9 SEM micrograph of an LSCF layer produced with a 10% N_2 plasma flowing at 250 slpm with an arc current of 150 A per cathode and a nozzle size of 1/2″ (~12.7 mm)

Acknowledgments

The authors gratefully acknowledge the financial support of the Natural Science and Engineering Research Council of Canada (NSERC) and of Northwest Mettech Corporation. Additionally, the authors acknowledge the support of the Solid Oxide Fuel Cell Canada Strategic Research Network from NSERC and other sponsors listed at www.sofccanada.com.

References

1. B.D. White and O. Kesler, Air Plasma Spraying of LSM/YSZ SOFC Composite Cathodes, *THERMEC 2006, 5th International Conference on Processing & Manufacturing of Advanced Materials*, T. Chandra, K. Tsuzaki, M. Militzer, and C. Ravindran, Ed., July 3-8, 2006 (Vancouver, BC, Canada), Trans Tech Publications Inc., 2007, p 299-304
2. X. Zhang, C. Deces-Petit, S. Yick, M. Robertson, O. Kesler, R. Maric, and D. Ghosh, A Study on Sintering Aids for $Sm_{0.2}Ce_{0.8}O_{1.9}$ Electrolyte, *J. Power Sour.*, 2006, **162**(1), p 480-485
3. O. Kesler, Plasma Spray Processing of Solid Oxide Fuel Cells, *Mater. Sci. Forum*, 2007, **539-543**, p 1385-1390

4. B. White, O. Kesler, and L. Rose, Electrochemical Characterization of Air Plasma Sprayed LSM/YSZ Composite Cathodes on Metallic Interconnects, *ECS Trans.*, 2007, **7**(1), p 1107-1114
5. B.D. White, O. Kesler, and L. Rose, Air Plasma Sprayed Processing and Electrochemical Characterization of SOFC Composite Cathodes, *J. Power Sour.*, 2008, **178**(1), p 334-343
6. Y. Teraoka, H.M. Zhang, K. Okamoto, and N. Yamazoe, Mixed Ionic-Electronic Conductivity of $La_{1-x}Sr_xCo_{1-y}Fe_yO_{3-\delta}$ Perovskite-Type Oxides, *Mater. Res. Bull.*, 1988, **23**(1), p 51-58
7. I.A. Raj, A.S. Nesaraj, M. Kumar, F. Tietz, H.P. Buchkremer, and D. Stöver, On the Suitability of $La_{0.60}Sr_{0.40}Co_{0.20}Fe_{0.80}O_3$ Cathode for the Intermediate Temperature Solid Oxide Fuel Cell (ITSOFC), *J. New Mater. Electrochem. Syst.,* 2004, **7**(2 special issue), p 145-151
8. K.K. Hansen and K.V. Hansen, A-Site Deficient $(La_{0.6}Sr_{0.4})_{1-s}Fe_{0.8}Co_{0.2}O_{3-\delta}$ Perovskites as SOFC Cathodes, *Solid State Ion.*, 2007, **178**, p 1379-1384
9. K. Kammer, Studies of Fe-Co Based Perovskite Cathodes with Different A-site Cations, *Solid State Ion.*, 2006, **177**(11-12), p 1047-1051
10. A. Mai, V.A.C. Haanappel, S. Uhlenbruck, F. Tietz, and D. Stöver, Ferrite-Based Perovskites as Cathode Materials For Anode-Supported Solid Oxide Fuel Cells, *Solid State Ion*, 2005, **176**(15-16), p 1341-1350
11. F. Tietz, Q. Fu, V.A.C. Haanappel, A. Mai, N.H. Menzler, and S. Uhlenbruck, Materials Development for Advanced Planar Solid Oxide Fuel Cells, *Int. J. Appl. Ceram. Technol.*, 2007, **4**, p 436-445
12. F. Tietz, V.A.C. Haanappel, A. Mai, J. Mertens, and D. Stöver, Performance of LSCF Cathodes in Cell Tests, *J. Power Sour.*, 2006, **156**, p 20-22
13. S. Bebelis, N. Kotsionopoulos, A. Mai, D. Rutenbeck, and F. Tietz, Electrochemical Characterization of Mixed Conducting and Composite SOFC Cathodes, *Solid State Ion.*, 2006, **177**(19-25), p 1843-1848
14. C. Fu, K. Sun, N. Zhang, X. Chen, and D. Zhou, Electrochemical Characteristics of LSCF-SDC Composite Cathode for Intermediate Temperature SOFC, *Electrochim. Acta*, 2007, **52**(13), p 4589-4594
15. E.P. Murray, M.J. Sever, and S.A. Barnett, Electrochemical Performance of $(La,Sr)(Co,Fe)O_3$-$(Ce,Gd)O_3$ Composite Cathodes, *Solid State Ion.*, 2002, **148**, p 27-34
16. W.G. Wang and M. Mogensen, High-Performance Lanthanum-Ferrite-Based Cathode for SOFC, *Solid State Ion.*, 2005, **176**(5-6), p 457-462
17. J. Lagerbom, A. Nikkilä, M. Kylmälahti, P. Vuoristo, U. Kanerva, and T. Varis, Phase Stability and Structure of Conductive Perovskite Ceramic Coatings by Thermal Spraying, *Thermal Spray: Crossing Borders*, E. Lugscheider, Ed., June 2-4, 2008 (Maastricht, The Netherlands), ASM International, 2008, p 1103-1108
18. A.A. Syed, Z. Ilhan, and G. Schiller, Plasma Sprayed Oxygen Electrode for Solid Oxide Fuel Cells and High Temperature Water Electrolyzers, *Thermal Spray: Crossing Borders*, E. Lugscheider, Ed., June 2-4, 2008 (Maastricht, The Netherlands), ASM International, 2008, p 190-194
19. S. Park, S. Kumar, H. Na, and C. Lee, Effects of Silver Addition on Properties and Performance of Plasma Sprayed $La_{0.6}Sr_{0.4}$-$Co_{0.2}Fe_{0.8}O_{3-\delta}$ Interconnect Layer, *J. Therm. Spray Technol.,* 2008, **17**, p 1-7
20. J. Oberste Berghaus, J. Legoux, C. Moreau, R. Hui, and D. Ghosh, Suspension Plasma Spraying of Intermediate Temperature SOFC Components Using an Axial Injection DC Torch, *Mater. Sci. Forum*, 2007, **539-543**, p 1332-1337
21. D. Waldbillig, Z. Tang, A. Burgess, and O. Kesler, Effect of Substrate and Cathode Parameters on the Properties of Suspension Plasma Sprayed Solid Oxide Fuel Cell Electrolytes, *Thermal Spray: Crossing Borders*, E. Lugscheider, Ed., June 2-4, 2008 (Maastricht, The Netherlands), ASM International, 2008, p 201-206
22. C. Monterrubio-Badillo, H. Ageorges, T. Chartier, J.F. Coudert, and P. Fauchais, Preparation of $LaMnO_3$ Perovskite Thin Films by Suspension Plasma Spraying for SOFC Cathodes, *Surf. Coat. Technol.*, 2006, **200**(12-13), p 3743-3756